ChemPhysChem

Research Article
doi.org/10.1002/cphc.202200343

Chemistry Europe
European Chemical Societies Publishing

www.chemphyschem.org

On the Notation of Catastrophes in the Framework of Bonding Evolution Theory: Case of Normal and Inverse Electron Demand Diels-Alder Reactions

Leandro Ayarde-Henríquez,*[a] Cristian Guerra,[a] Mario Duque-Noreña,[a, b] Elizabeth Rincón,[c] Patricia Pérez,*[a, b] and Eduardo Chamorro*[a, b]

This paper generalizes very recent and unexpected findings [*J. Phys. Chem. A*, **2021**, *125*, 5152–5165] regarding the known "direct- and inverse-electron demand" Diels-Alder mechanisms. Application of bonding evolution theory indicates that the key electron rearrangement associated with significant chemical events (e.g., the breaking/forming processes of bonds) can be characterized via the simplest fold polynomial. For the CC bond formation, neither substituent position nor the type of electronic demand induces a measurable cusp-type signature. As opposed to the case of [4+2] cycloaddition between 1,3-butadiene and ethylene, where the two new CC single bonds occur beyond the transition state (TS) in the activated cases, the first CC bond occurs in the domain of structural stability featuring the TS, whereas the second one remains located in the deactivation path connecting the TS with the cycloadduct.

Introduction

It has been recently evidenced that bonding events implied in the prototypical Diels-Alder (DA) reaction between ethylene and 1,3-butadiene can be rationalized in terms of the fold elementary catastrophe (Scheme 1).[1]

This observation derives from Thom's elementary catastrophe theory[2] to the evolution of the phase-space portrait (i.e., the molecular graph) derived from the topological analysis of the electron localization function (ELF).[3] Within such a framework defining the so-called bonding evolution theory (BET),[4] any reaction mechanism can be understood in terms of electron pairing changes featuring different structural stability domains (SSDs)[2,5–7] separated by catastrophe bifurcations.[2] Hence, we have emphasized that the correct determination of the type of catastrophe must be based on examining the determinant of the Hessian matrix and the relative distance between critical points along the reaction path.[1]

Seven SSDs separated by ten catastrophes can be identified as specific signatures for such a single-step reaction mechanism

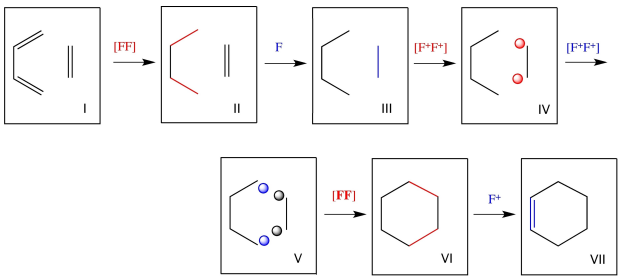

Scheme 1. Simplified Lewis-type formula representation (excluding hydrogen atoms) based on ELF topology for the sequence of electronic stages implied along the one-step mechanism of the Diels-Alder reaction between 1,3-butadiene and ethylene to yield cyclohexene. BET analysis reveals that all bifurcations separating the seven structural stability domains I–VII (including those associated with the onset of the CC bonds formation) are of fold type.

featuring the DA reaction.[1] Surprisingly, no flags for cusp bifurcations have been detected along the intrinsic reaction path (IRC),[8] even in the region where the two new CC bonds are formed.[1] As described through the IRC, the reaction mechanism should imply a sequence of only fold catastrophes, i.e., the simplest unfolding within the framework of elementary catastrophe theory (ECT).[2]

The importance of this finding is that *we can choose only one "external" parameter (e.g., related to the reaction coordinate space) to describe each bonding change event along the entire process.*[1] Moreover, given the inherent asymmetry of the electron distribution in most of the implied fragments in a chemical reaction, fold catastrophes can always be expected from such a framework. Cusp catastrophes (or even higher dimensional ones) might be entirely associated with highly symmetrical conditions, such as any perfectly represented homolytic bond rupture/formation implying completely equivalent reactive fragments. Indeed, such a working hypothesis has

[a] *Dr. L. Ayarde-Henríquez, Dr. C. Guerra, Prof. Dr. M. Duque-Noreña, Prof. Dr. P. Pérez, Prof. Dr. E. Chamorro*
Departamento de Ciencias Químicas
Universidad Andrés Bello
Avenida República 275,
Santiago de Chile, Chile
E-mail: l.ayardehenriquez@uandresbello.edu
p.perez@unab.cl
echamorro@unab.cl
[b] *Prof. Dr. M. Duque-Noreña, Prof. Dr. P. Pérez, Prof. Dr. E. Chamorro*
Centro de Química Teórica y Computacional
Universidad Andrés Bello
Avenida República 275
Santiago de Chile, Chile
[c] *Prof. Dr. E. Rincón*
Instituto de Ciencias Químicas
Universidad Austral de Chile
Las encinas 220, Valdivia, Chile

been recently tested in both ground-[1] and excited-state[9–11] reaction processes.

Note that in a BET context of rationalization, which is based on the ELF and ECT formalisms, the interatomic distance between the implied carbon centres can always be chosen as the single control parameter featuring the fold catastrophe, *allowing us adequately to describe all the abrupt bifurcations in the phase space that are associated with chemically significant bond formation/bond rupture events.*[1] Following ongoing interests related to the elucidation of DA processes, in this work, we explore electron-donor (ED) and electron-withdrawing (EW) substituent effects on ethylene and 1,3-butadiene encompassing examples of the so-called normal electron demand (NED) and inverse electron demand (IED) in DA cycloaddition reactions (Scheme 2).

The form that catastrophe signatures vary in function of the electronic nature of the reactants is undoubtedly a crucial subject that needs to be explored further. As the theoretical basis for the BET analysis is widely available in the literature,[1,4,9–16] we only recall the required general details in the **Theoretical and Computational Section**.

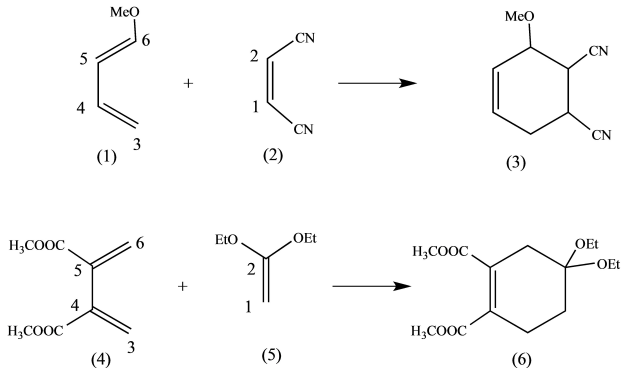

Scheme 2. DA reactions studied in the present work exemplifying direct demand (1 + 2 → 3) and inverse demand (4 + 5 → 6) electronic processes; i.e., 1–methoxy–1,3–butadiene (1) with butenedinitrile (2) to yield 3-methoxy-4-cyclohexene-1,2-dicarbonitrile (3); and 1,4-Dimethyl 2,3-bis(methylene)butanedioate (4) with 1,1-diethoxyethene (5) to yield 1,2-dimethyl 4,4-diethoxy-1-cyclohexene-1,2-dicarboxylate (6), respectively.

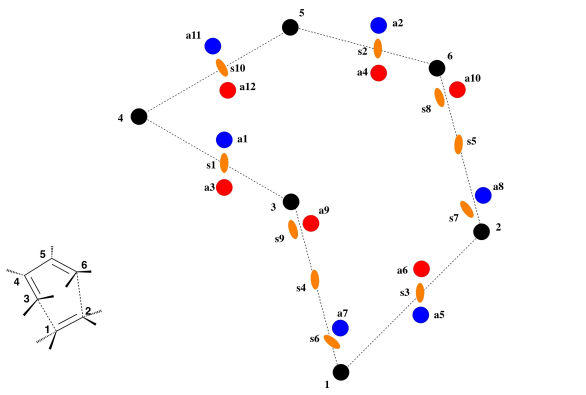

Scheme 3. Simplified representation for the [2+4] reaction center of the DA reactions studied in this work. BET analysis reveals that all bifurcations separating the seven structural stability domains I–X (including those associated with the onset for the formation of the C1-C3 and C2-C6 bond formations) are of fold type. The implied maxima and saddles are represented by circles in violet and orange colors, respectively.

Results and Discussion

The topological analysis of ELF for both reactions allows us to fully characterize the complete set of critical points for each configuration along the pathway. In each case, *we have been able to identify bifurcations that involve collisions between attractors or (3,–3) and saddles of index one or (3,–1) Morse critical points as the origin of degeneration leading to the change of ELF topology along the studied reaction paths.* Scheme 3 briefly reports, unifying the labels, those maxima and saddle critical points associated with the reaction center of the [4+2] DA studied reactions.

Direct Electron Demand: Nature of Bonding along the DA Reaction between 1–methoxy–1,3–butadiene (1) and butenedinitrile (2)

The (1)+(2)→(3) reaction process implies nine SSDs separated by ten catastrophes. The first change in the topographic map is associated with the C3=C4 double bond region of the diene (1) and separates the SSD–I from SSD-II. Such a bifurcation arises from the annihilation of the attractor a3 with the saddle s1 yielding a wandering point (wp), i.e., a3+s1→wp. The attractor a1, in the C3=C4 region, remains along the bifurcation originating the disynaptic basin V(C3,C4). This first bifurcation is a fold in type within Thom's catastrophe theory and features the onset of the "reduction" of the C3=C4 double bond character. The second bifurcation separates SSD-II from SSD-III and occurs at the diene (1) at the C5=C6 double bond region. The fold bifurcation a4+s2→wp now signs the change in topology. The third bifurcation occurs in the C1=C2 double bond region of the butenedinitrile specie (2) and separates SSD-III from SSD-IV. Again, this event is related to a fold bifurcation namely, a6+s3→wp. Henceforth, and as previously observed, no cups catastrophes seem to be implied in the "activation" process of the double bond regions of this [4+2] DA reaction. However, in contrast to the case of the DA mechanism between 1,3-butadiene and ethylene, the catastrophes at the double bond regions of the 1–methoxy–1,3–butadiene (1) are not simultaneous. The next three bifurcations occur in sequential order and separate the SSD-IV, SSD–V, SSD-VI, and SSD-VII, along the IRC. These correspond with the apparition of attractors a7, a8, and a9, and saddles s6, s7, and s9 in the vicinity of carbons C1, C2, and C3, respectively. These define the fourth, fifth and sixth bifurcations, i.e., wp→a7+s6, wp→a8+s7, and wp→a9+s9, respectively, fold in terms of Thom's classification. Maxima a7, a8, and a9 define monosynaptic basins, which are associated with the concentration of electron density in the regions of terminal carbon centers in both interacting species. Some authors agree in describing these events as a polarization effect, and in the present case,

these have to be related to the electron donor character of the methoxy group substitution in the diene fragment (1) and the electron-withdrawing effect of the CN groups at the dienophile (2). It should be emphasized that these "preparative" electronic events occur before the reacting system reaches the transition structure (TS). The seventh catastrophe separates SDD-VI from SSD-VII, which constitutes the onset of the process leading to the formation of the new C1–C3 single bond, and indeed features the topology of the TS along the SSD-VII. As earlier evidenced by the prototypical DA reaction, this event is also a fold catastrophe, namely a9 + s4→wp. In such a context, the attractor that remains and provides the new disynaptic V(C1,C3) basin corresponds to the maxima a7, which originated in the vicinity of the C1 center due to the fourth bifurcation. The concurrent eighth and ninth bifurcations occur along the "deactivation" pathway separating SSD-VII from SSD-VIII. Both correspond to fold processes wp→a12 + s10, and wp→a10 + s8, becoming associated with the subsequent accumulation of electron density at the C4-C5 bond region and the C6 center. Finally, the tenth fold catastrophe, separating SSD-VIII from SDD-IX, is associated with the topological changes cantered at the C2-C6 bonding region, which yields to the forming of the CC single bond and the final closure of the ring, namely a10 + s5→wp. The attractor that remains corresponds to the earlier one originated at the C2, i.e., a8, which creates the new disynaptic V(C2,C6) basin in the cycloadduct (3). Scheme 4 summarizes via Lewis-type formulas the sequence of SSDs implied along the single step for the (1) + (2)→(3) process, as described through the IRC.

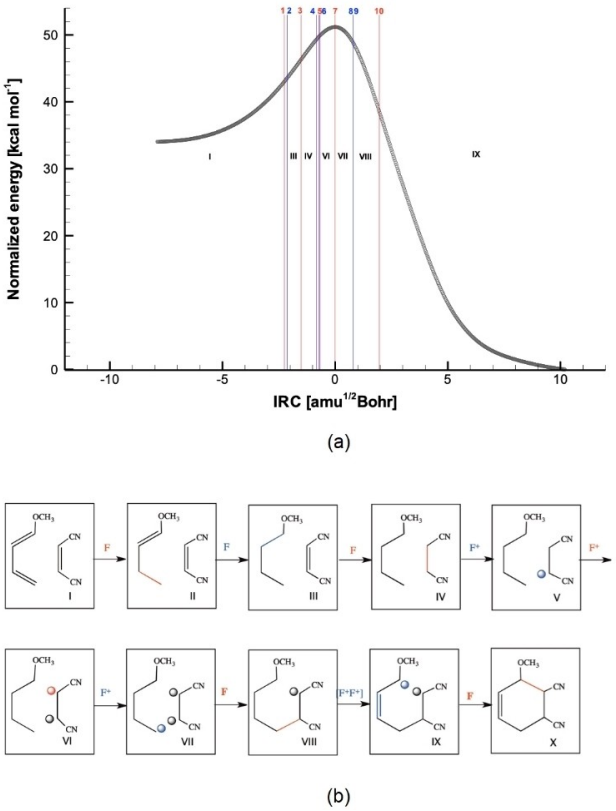

Scheme 4. (a) Intrinsic reaction coordinate (IRC) plot of the transition state of the Diels-Alder reaction between 1–methoxy–1,3–butadiene (1) with butenedinitrile (2) obtained at the ωB97X-D/6-31G(d) level of theory. Integer numbers indicate the location of catastrophe bifurcations dividing the IRC space. The BET analysis reveals the existence of nine structural stability domains I–IX. (b) Simplified Lewis-type formula representation (excluding hydrogen atoms) based on ELF for the sequence of electronic stages implied along the single-step reaction. All bifurcations (even those associated with the onset of the C–C bonds formation) are of fold type.

Inverse Electron Demand: Nature of Bonding along the DA Reaction between 1,4-Dimethyl 2,3-bis(methylene)butanedioate (4) and 1,1-Diethoxyethene (5)

Scheme 5 summarizes via Lewis-type formulas the sequence of SSDs implied along the one-step mechanism of the inverse electron demand DA reaction between (4) and (5). In this case, the first and second main topological changes are centered in the C3 = C4 unsaturated bonding region of the electron-deficient diene fragment and on the C1 = C2 bonding region in the activated dienophile. Both bifurcations are fold in type, implying the annihilation of an attractor and a saddle of index 1, namely a3 + s1→wp, and a6 + s3→wp, respectively. The attractors a1 and a5 originates the valence disynaptic basins V(C3,C4) and V(C1,C2). Such events correspond to the onset of the asymmetric reduction of unsaturated bonding regions in the reaction partners.

The creation of maxima and saddles of index 1 in the neighbourhoods of C1 and C3 defines the third and fourth catastrophes. In both cases, the new attractor and saddle point originate from a wandering point, i.e., wp→a7 + s6, and wp→a9 + s9, respectively, corresponding also to fold signatures.

The subsequent fifth bifurcation marks the onset of the electron reorganization processes leading to the C1–C3 single bond formation, namely a9 + s4→wp, which features the SSD-VI (i.e., the topology of the TS belongs to such a domain). It is the attractor a7 that evolves as the origin of the valence disynaptic V(C1,C3) basin. The formation of the C1–C3 single bond should therefore be characterized as a fold–type catastrophe. As was the case for the direct electron demand process, the formation of the first CC bond is also located at the top of the barrier.

The sixth change in the ELF shape separates the SSD-VI from the SSD-VII and occurs in the molecular space of the double bond between C5 = C6, i.e., a4 + s2→wp. The attractor a2 is not involved in the bifurcation and will define the valence disynaptic V(C5,C6) basin. The seventh catastrophe features the fold processes wp→ a10 + s8 near C6. The eighth and ninth catastrophes originate in sequence from the wp→ a8 + s7 and wp→ a12 + s10 fold processes occurring in the locality of C2 and within the C4–C5 bond region, respectively.

The attractor a11 displays no flag of degeneration, and the simplest Thom's polynomial provides a solid description for the C4 = C5 double bond formation. The last bifurcation constitutes the onset of the cyclic product formation due to the merging of a10 and s5, featuring a fold bifurcation, i.e., a8 + s5→wp, and the attractor a10 originating the new disynaptic basin V(C2,C6).

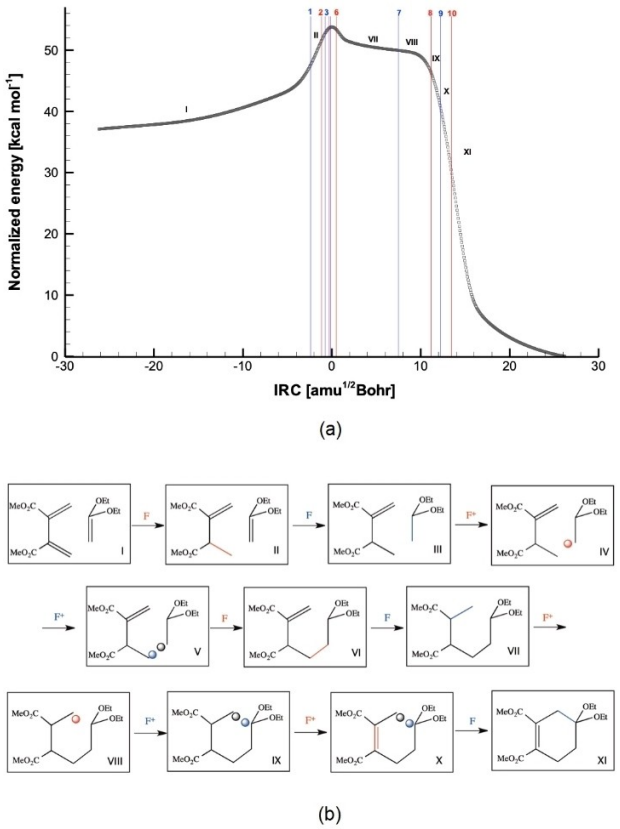

Scheme 5. (a) Intrinsic reaction coordinate (IRC) plot of the transition state of the Diels-Alder reaction between dimethyl 2,3–dimethylenesuccinate (4) with 1,1-diethoxyethene (5) obtained at the ωB97X-D/6-31G(d) level of theory. Integer numbers indicate the location of catastrophe bifurcations dividing the IRC space. The BET analysis reveals the existence of eleven structural stability domains I–XI. (b) Simplified Lewis-type formula representation (excluding hydrogen atoms) based on ELF for the sequence of electronic stages implied along the single-step reaction. All bifurcations (even those associated with the onset of the C–C bonds formation) are of fold type.

Within the framework of a chemical interpretation, one is tempted to describe the electron-pair reorganizations featuring both reaction systems within the so-called arrow-pushing model (i.e., curly arrow diagrams).[17] Since the values of the Hessian matrix at potentially degenerated CPs and the relative distance between such points show that the fold polynomial characterizes both the bond-breaking and bond-forming, it will suffice to discuss only one event, for instance, any of the bifurcation leading to a new sigma bond. From a topographical viewpoint, this means that one of the ELF maxima collides with a saddle of index one, and both CPs disappear, implying that the electron-pair density flows from the basin associated with this attractor and accumulates in the basin of the remaining one, as also evidenced for the hydrogen-substituted DA reaction.[1] The arrow-model description of this chemical process will demand one curved arrow to represent the ''jump'' of the electron population from one basin to the other. In contrast, a completely different picture would result if this event were described in terms of a cusp-type function[18] because, in such a case, two curly arrows would be required. The present BET results will stress the need for a systematic analysis of the curly arrow model and its fuzzy connection with electron flow concepts and the rationalization of reaction mechanisms.

Conclusions

The evolution of the topology of the electron localization function along the intrinsic reaction coordinate for simple representative examples of both direct and inverse demand examples of Diels-Alder reactions is described above. The topological picture establishes two main separated stages, namely C1–C3 (starting at the TS configuration) and C2–C6 formation located on the deactivation path connecting the TS and cycloadduct. The nonconcerted mechanistic rationalization has been described as a one-step two-stages process. That is, just one kinetic step, and two key (electronic) stages/events referred to the formation of the new CC single bonds. In contrast, in the case of prototypical [4 + 2] cycloaddition between 1,3-butadiene and ethylene, the topological signature of the two new CC single bonds occurs simultaneously on the deactivation path, beyond the TS configuration. Notably, here again, only fold catastrophes are implied. This fact further supports our working hypothesis, given that the enhanced electron demand (originated by the substitution pattern) introduces a higher degree of asymmetry of electron density in the bonding regions. Thus, although the bifurcation sequence in the substituted cases differs from the prototypical (i.e., hydrogen substituted) DA reaction, the nature of topological signatures (based on the application of BET methodology) remains identical. It has been argued that the changes in the ELF topology along the IRC can be chemically understood using VSEPR-like considerations.[17] In principle, it would also lead to accurate qualitative predictions regarding the studied DA reactions. Note that ELF enables the separation of valence and core electronic pair domains, and the interplay between nuclei rearrangement and the valence electronic reorganization drive the course of a chemical transformation as elucidated through a reaction path. BET enables a straightforward procedure to establish what type of bond is first formed and its location along the chosen reaction coordinate. It is certainly quite surprisingly the simplest polynomial of Thom's catastrophe theory describes all the significant chemical events, such as the breaking and forming processes of chemical bonds. This means that only one parameter is needed to describe inter and intramolecular changes along the chosen reaction coordinate. The selection of the control parameter become greatly simplified. These findings open several questions regarding the specific conditions needed to identify any signature of a higher dimensional bifurcation (e.g., cusp elementary catastrophe) in pericyclic reactions. Could they be general enough to apply to other types of reactions if those conditions exist?. This work leads to a paradigm change concerning the topological description of significant events such as the breaking and forming of chemical bonds and suggests that systems explored within the original version of the bonding evolution theory over the last 25 years should be re-examined.

Theoretical and Computational Section

The partition of the molecular space into basins of attractors (maxima) can be associated with chemically significant concepts of bonding through the topological analysis of suitable local functions.[19–23] Structures derived from this analysis are specified in the form of critical points (CPs) and their interconnections via gradient paths.[22] Within this framework, QTAIM[25] and ELF,[3] are nowadays useful methodological tools that help us rationalize concepts related to chemical bonding.[15,25,26] Bonding evolution theory,[4] which combines the topological analysis of ELF with Thom's catastrophe theory,[2] has permitted exploring chemical reactions as sequences of SSDs in processes involving rupture/formation bonds.[1,4,9–11,15] Any chemical reaction involving covalent bonds within the BET approach can be represented by a succession of catastrophic bifurcations associated with electron pairing topologies for a simple rationalization of the chemical bonding patterns. Besides the sequence of molecular graphs (given by number and type of CPs) to characterize a catastrophe, it is also necessary to examine the Morse critical points (i.e., maxima, saddles, and minima) in the vicinity of the catastrophe.[1,9–11] As a result, a complete BET entails a thorough examination of the Hessian matrix determinant and the corresponding relative distance between CPs of ELF along the reaction path.[1]

Geometry optimizations and associated stationary point characterization were conducted at the ωB97X-D/6-31G(d) level of theory using the Gaussian16[27] package of programs. *As previously evidenced using the functionals B3LYP, KMLYP, M06-2X, MPWB1 K, and ωB97X-D, topological properties (as required for the BET analysis of DA processes) and bifurcation flags do not depend on the level of the theory.*[1] Optimized Cartesian coordinates for reactants, transition structures, products, and animated sequences of catastrophes are available (see the Supporting Information). The IRC paths for both reactions depicted in Scheme 2 were evaluated using a step size equal to 0.002 amu$^{1/2}$Bohr. The paths for the direct and inverse demand paths involved 501 and 801 points along the IRC path, respectively. The topological analysis of ELF and the characterization of the associated phase-space portrait at each point incorporating the four types of CPs was performed by using the Multiwfn[28] and VMD[29] program suites. For each molecular configuration along the path, the fulfillment of the Poincaré-Hopf theorem[30] has been strictly verified. The nature of all catastrophe bifurcations was established by examining the absolute value of the determinant of the Hessian matrix evaluated at the Morse critical points and their relative positions in the neighborhoods of the degeneration.

Acknowledgements

The authors acknowledge the ANID/CONICYT Ph.D. scholarship awarded to L.A.-H. We also are indebted to the Fondo Nacional de Ciencia y Tecnología (FONDECYT-ANID, Chile), by the continuous financial and academic support provided through Project Nos. 1181582 (E.C.) and 1221383 (P.P.)

Conflict of Interest

The authors declare no conflict of interest.

Data Availability Statement

The data that support the findings of this study are available from the corresponding author upon reasonable request.

Keywords: Diels-Alder reactions · pericyclic reactions · normal and inverse electron demands · nonconcerted reaction mechanisms · Bonding evolution theory

[1] L. Ayarde-Henríquez, C. Guerra, M. Duque-Noreña, E. Rincón, P. Pérez, E. Chamorro, *J. Phys. Chem. A* **2021**, *125*, 5152–5165.
[2] R. Thom, *Structural Stability and Morphogenesis*, Taylor & Francis Group LLC, Florida **1972**.
[3] A. D. Becke, K. E. Edgecombe, *J. Chem. Phys.* **1990**, *92*, 5397–5403.
[4] X. Krokidis, S. Noury, B. Silvi, *J. Phys. Chem. A* **1997**, *101*, 7277–7282.
[5] R. Gilmore, *Catastrophe Theory for Scientists and Engineers*, Dover Publications, New York **1993**.
[6] T. Poston, I. Stewart, *Catastrophe Theory and its Applications*, Pitman Publishing Limited, London **1979**.
[7] D. Castrigiano, S. Hayes, *Catastrophe Theory*, CRC Press **2018**.
[8] K. Fukui, *J. Phys. Chem.* **1970**, *74*, 4161–4163.
[9] C. Guerra, L. Ayarde-Henríquez, M. Duque-Noreña, E. Chamorro, *J. Phys. Chem. A* **2022**, *126*, 395–405.
[10] C. Guerra, L. Ayarde-Henríquez, M. Duque-Noreña, C. Cárdenas, P. Pérez, E. Chamorro, *Phys. Chem. Chem. Phys.* **2021**, *23*, 20598–20606.
[11] C. Guerra, L. Ayarde-Henríquez, M. Duque-Noreña, E. Chamorro, *ChemPhysChem* **2021**, *22*, 2342–2351.
[12] J. Andrés, S. Berski, L. R. Domingo, V. Polo, B. Silvi, *Curr. Org. Chem.* **2011**, *15*, 3566–3575.
[13] J. Andrés, P. González-Navarrete, V. S. Safont, *Int. J. Quantum Chem.* **2014**, *114*, 1239–1252.
[14] J. Andrés, L. Gracia, P. González-Navarrete, V. S. Safont, *Comput. Theor. Chem.* **2015**, *1053*, 17–30.
[15] J. Andrés, P. González-Navarrete, V. S. Safont, B. Silvi, *Phys. Chem. Chem. Phys.* **2017**, *19*, 29031–29046.
[16] A. I. Adjieufacka, I. M. Ndassa, I. Patouossa, J. K. Mbadcam, V. S. Safont, M. Oliva, J. Andrés, *Phys. Chem. Chem. Phys.* **2017**, *19*, 18288–18302.
[17] J. Andrés, S. Berski, B. Silvi, *Chem. Commun.* **2016**, *52*, 8183–8195.
[18] S. Berski, J. Andrés, B. Silvi, L. R. Domingo, *J. Phys. Chem. A* **2003**, *107*, 6014–6024.
[19] A. Savin, A. D. Becke, J. Flad, R. Nesper, H. Preuss, H. G. von Schnering, *Angew. Chem. Int. Ed. Engl.* **1991**, *30*, 409–412.
[20] A. Savin, R. Nesper, S. Wengert, T. F. Fässler, *Angew. Chem. Int. Ed. Engl.* **1997**, *36*, 1808–1832.
[21] R. Bader, J. Hernández-Ttrujillo, F. Corstés-Guzmán, *J. Comput. Chem.* **2007**, *28*, 4–14.
[22] V. Polo, J. Andrés, *J. Comput. Chem.* **2005**, *26*, 1427–1437.
[23] P. L. A. Popelier, in *The Chemical Bond – 100 years old and getting stronger*, (Ed.: M. Mingo), Springer International Publishing Switzerland **2016**, pp. 71–118.
[24] R. Bader, *Atoms in Molecules: A Quantum Theory (International Series of Monographs on Chemistry)*, Clarendon Press Oxford, 1st edn. **1994**.
[25] J. Andrés, V. S. Safont, M. Oliva, K. L. Caster, F. Goulay, *Int. J. Quantum Chem.* **2022**, *122*, e26892.
[26] A. Savin, *J. Mol. Struct.: THEOCHEM* **2005**, *727*, 127–131.
[27] M. A. M. J. Frisch, G. W. Trucks, H. B. Schlegel, G. E. Scuseria, G. A. Robb, J. R. Cheeseman, G. Scalmani, V. Barone, B. Mennucci, J. B. Petersson, H. Nakatsuji, X. Li, M. Caricato, A. V. Marenich, J. V. O. B. G. Janesko, R. Gomperts, B. Mennucci, H. P. Hratchian, F. A. F. Izmaylov, J. L. Sonnenberg, D. Williams-Young, F. Ding, D. Lipparini, F. Egidi, J. Goings, B. Peng, A. petrone, T. Henderson, W. L. Ranasinhe, V. G. Zakrzewski, J. Gao, N. Rega, G. Zheng, T. M. Hada, M. Ehara, K. Toyota, R. Fukuda, J. Hasegawa, M. Ishida, J. A. Nakajima, Y. Honda, O. Kitao, H. Nakai, T. Vreven, K. Throssell, E. Montgomery Jr., J. E. Peralta, F. Ogliaro, M.

Bearpark, J. J. Heyd, R. K. N. Brothers, K. N. Kudin, V. N. Staroverov, T. A. Keith, S. S. I. J. Normand, K. Raghavachari, A. Rendell, J. C. Burant, J. J. Tomasi, M. Cossi, J. M. Millam, M. Klene, C. Adamo, R. Cammi, J. B. F. W. Ochterski, R. L. Martin, K. Morokuma, Ö. Farkas, D. J. Fox, Gaussian 16, Wallingford **2017**.
[28] T. Lu, F. Chen, *J. Comput. Chem.* **2012**, *33*, 580–592.
[29] K. S. W. Humphrey, A. Dalke, *J. Mol. Graphics* **1996**, *14*, 33–38.
[30] S. Albeverio, J. B. Alblas, S. A. Amitsur, I. J. Bakelman, G. Bakker, J. W. de Bakker, C. Bardos, H. Bart, H. Bass, A. Bensoussan, M. Bercovier, L. Berkovitz, M. Berger, E. A. Bergshoeff, E. Bertin, F. Beukers, A. Beutelspacher, H. P. Boas, J. Bochnak, H. J. M. Bos, B. L. J. Braaksma, T. P. Branson, D. S. Bridges, A. E. Brouwer, M. G. de Bruin, R. G. Bums, H. Capel, P. Cartier, C. Cercignani, J. M. C. Clark, Ph. Clement, A. M. Cohen, J. W. Cohen, P. Conrad, H. S. M. Coxeter, R. F. Curtain, M. H. A. Davis, M. V. Dekster, C. Dellacherie, G. van Dijk, H. C. Doets, I. Dolgachev, A. Dress, J. J. Duistermaat, D. van Dulst, H. van Duyn, H. Dym, A. Dynin, M. L. Eaton, W. Eckhaus, P. van Emde Boas, H. Engl, G. Ewald, V. I. Fabrikant, A. Fasano, M. Fliess, R. M. Fossum, B. Fuchssteiner, G. B. M. van der Geer, R. D. Gill, V. V. Goldberg, J. de Graaf, J. Grasman, P. A. Griffith, A. W. Grootendorst, L. Gross, P. Gruber, K. P. Hart, G. Heckman, A. J. Hermans, W. H. Hesselink, C. C. Heyde, M. W. Hirsch, K. H. Hofmann, A. T. de Hoop, P. J. van der Houwen, N. M. Hugenholtz, J. R. Isbell, A. Isidori, E. M. de Jager, D. Johnson, P. T. Johnstone, D. Jungnickel, M. A. Kaashoek, V. Kac, W. L. J. van der Kallen, D. Kanevsky, Y. Kannai, H. Kaul, E. A. de Kerf, W. Klingenberg, T. Kloek, J. A. C. Kolk, G. Komen, T. H. Koomwinder, L. Krop, B. Kuperschmidt, H. A. Lauwerier, J. va Leeuwen, H. W. Lenstra Jr., J. K. Lenstra, H. Lenz, M. Levi, J. Lindenstrauss, J. H. van Lint, F. Linton, A. Liulevicius, M. Livshits, W. A. J. Luxemburg, R. M. M. Mattheij, L. G. T. Meertens, I. Moerdijk, J. P. Murre, H. Neunzert, G. Y. Nieuwland, G. J. Olsder, B. Orsted, F. van Oystaeyen, B. Pareigis, K. R. Parthasarathy, K. R. Parthasarathy, 1.1. Piatetskii-Shapiro, H. G. J. Pijls, N. U. Prabhu, E. Primrose, A. Ramm, C. M. Ringel, J. B. T. M. Roerdink, K. W. Roggenkamp, G. Rozenberg, W. Rudin, S. N. M. Ruysenaars, A. Salam, A. Salomaa, P. Saunders, J. P. M. Schalkwijk, C. L. Scheffer, R. Schneider, J. A. Schouten, F. Schurer, J. J. Seidel, A. Shenitzer, V. Snaith, T. A. Springer, J. H. M. Steenbrink, J. D. Stegeman, F. W. Steutel, P. Stevenhagen, I. Stewart, R. Stong, L. Streit, K. Stromberg, L. G. Suttorp, D. Tabak, F. Takens, R. J. Takens, N. M. Temme, S. H. Tijs, B. Trakhtenbrot, N. S. Tmdinger, L. N. Vaserstein, M. L. J. van de Vel, F. D. Veldkamp, W. Vervaat, P. M. B. Vitanyi, N. J. Vlaar, H. A. van der Vorst, J. de Vries, F. Waldhausen, B. Wegner, J. J. O. O. Wiegerinck, J. C. Willems, J. M. Wills, B. de Wit, S. A. Wouthuysen, S. Yuzvinskii, L. Zalcman, *Encyclopaedia of Mathematics*, Vol. 7, (Ed.: I. M. Vinogradov), Kluwer Academic Publishers, Dordrecht **1991**.

Manuscript received: May 19, 2022
Revised manuscript received: July 8, 2022
Accepted manuscript online: July 16, 2022
Version of record online: ■■, ■■■

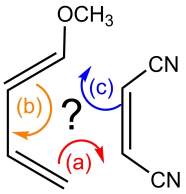

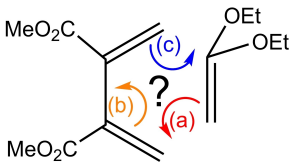

Dr. L. Ayarde-Henríquez, Dr. C. Guerra, Prof. Dr. M. Duque-Noreña, Prof. Dr. E. Rincón, Prof. Dr. P. Pérez*, Prof. Dr. E. Chamorro**

1 – 7

On the Notation of Catastrophes in the Framework of Bonding Evolution Theory: Case of Normal and Inverse Electron Demand Diels-Alder Reactions

Interconnection between fold catastrophes and the asymmetry of the electron-pair density along a reaction pathway is independent of the electron-demand type and substituents. This questions the use of topological fingerprint for characterizing such reacting systems.